Unpredicted Scaling of the One-Dimensional Kardar-Parisi-Zhang Equation

Côme Fontaine,[1] Francesco Vercesi,[1] Marc Brachet,[2] and Léonie Canet[1,3]
[1]*Université Grenoble Alpes, CNRS, LPMMC, 38000 Grenoble, France*
[2]*Université PSL, CNRS, Sorbonne Université, Université de Paris, LPENS, 75005, Paris, France*
[3]*Institut Universitaire de France, 75000 Paris, France*

(Received 16 May 2023; accepted 17 November 2023; published 14 December 2023)

The celebrated Kardar-Parisi-Zhang (KPZ) equation describes the kinetic roughening of stochastically growing interfaces. In one dimension, the KPZ equation is exactly solvable and its statistical properties are known to an exquisite degree. Yet recent numerical simulations in the tensionless (or inviscid) limit of the KPZ equation [C. Cartes *et al.*, The Galerkin-truncated Burgers equation: Crossover from inviscid-thermalized to Kardar–Parisi–Zhang scaling, Phil. Trans. R. Soc. A **380**, 20210090 (2022).; E. Rodríguez-Fernández *et al.*, Anomalous ballistic scaling in the tensionless or inviscid Kardar-Parisi-Zhang equation, Phys. Rev. E **106**, 024802 (2022).] unveiled a new scaling, with a critical dynamical exponent $z = 1$ different from the KPZ one $z = 3/2$. In this Letter, we show that this scaling is controlled by a fixed point which had been missed so far and which corresponds to an infinite nonlinear coupling. Using the functional renormalization group (FRG), we demonstrate the existence of this fixed point and show that it yields $z = 1$. We calculate the correlation function and associated scaling function at this fixed point, providing both a numerical solution of the FRG equations within a reliable approximation, and an exact asymptotic form obtained in the limit of large wave numbers. Both scaling functions accurately match the one from the numerical simulations.

DOI: 10.1103/PhysRevLett.131.247101

The Kardar-Parisi-Zhang (KPZ) equation is remarkable for the large variety of systems in which it arises. Originally derived to model the kinetic roughening of stochastically growing interfaces [1], the KPZ equation has turned out to describe the universal properties of systems as different as various growing interfaces [2–5], equilibrium disordered systems [6], or turbulence in infinitely compressible fluids [7]. Perhaps even more striking is its recent observation in purely quantum systems, such as exciton-polariton condensates [8] or Heisenberg quantum spin chains [9,10]. The ubiquity of the KPZ equation promotes it to a fundamental model for nonequilibrium critical phenomena and phase transitions [11–14].

After more than two decades of intense efforts both in the mathematics and statistical physics communities, the one-dimensional (1D) KPZ equation has been solved exactly, and its statistical properties are now extensively charted [15]. In 1D, the critical exponents of the KPZ equation, roughness exponent χ and dynamical exponent z, are fixed by the symmetries to the exact values $\chi = 1/2$ and $z = 3/2$. The two-point correlation function has been calculated exactly [16]. The probability distribution of the KPZ height fluctuations is known, and reveals a sensitivity to the global geometry of the interface, while unveiling a deep connection with random matrix theory [15]. Many other properties are also known, such as the short-time behavior or the large deviation theory, to cite a few. However, the 1D KPZ equation still reserves its surprises.

In a recent paper [17], the authors performed numerical simulations of the 1D Burgers equation [18], which exactly maps to the KPZ equation, and studied the limit of vanishing viscosity (inviscid limit). They unveiled a crossover to a new scaling regime, characterized by a dynamical exponent $z = 1$, different from the KPZ value $z = 3/2$. The same result was reported in [19] in the equivalent tensionless limit of the KPZ equation, and also in [20] in a strongly interacting 1D quantum bosonic system. This scaling is absent in the current understanding of the 1D KPZ equation. In this Letter, we fill this gap, and provide the theoretical explanation of this missing scaling, using the functional renormalization group (FRG). In the renormalization group framework, the KPZ scaling is controlled by a fixed point, termed the KPZ fixed point. Another fixed point exists, the Edwards-Wilkinson (EW) fixed point, which corresponds to the KPZ equation with vanishing nonlinearity [21]. We show that the tensionless or inviscid limit of the KPZ equation is controlled by a third unexplored fixed point, which features the $z = 1$ critical dynamical exponent. We calculate the scaling function at this fixed point, and show that it very accurately coincides with the scaling function computed in the numerics.

Let us first justify on simple grounds the existence of this third fixed point. The KPZ equation gives the dynamics of a real-valued height field $h(t, \mathbf{x})$ with $\mathbf{x} \in \mathbb{R}^d$:

$$\partial_t h = \nu \nabla^2 h + \frac{\lambda}{2} (\boldsymbol{\nabla} h)^2 + \sqrt{D} \eta \tag{1}$$

where ν, λ, and D are three real parameters and η is a Gaussian noise of zero mean and correlations $\langle\eta(t,\mathbf{x})\eta(t',\mathbf{x}')\rangle = 2\delta(t-t')\delta^d(\mathbf{x}-\mathbf{x}')$. In fact, by rescaling the time and the field, one can show that this equation only depends on one parameter $g \equiv \lambda^2 D/\nu^3$ (or equivalently on the Reynolds number in the context of the Burgers equation). Note that we assume, as in [17], the existence of an UV cutoff scale, such that the solutions of (1) remain well defined in the inviscid limit and thermalize to the equilibrium distribution [17,22].

Within the RG framework, following Wilson's original idea, one progressively averages out fluctuations, shell by shell in wave numbers, starting from the high (ultraviolet UV) wave number modes [23]. One thus obtains the effective theory for the low (infrared IR) wave number modes, i.e., at large distances. When the system is scale invariant, this corresponds to a fixed point of the RG flow. Thus, the KPZ rough interface is described by an IR fixed point, the KPZ one, which is fully attractive in 1D and is characterized by $z = 3/2$ and $\chi = 1/2$.

At zero nonlinearity $\lambda = g = 0$, the Eq. (1) becomes the EW equation, and there exists the corresponding fixed point describing the linear system, characterized in 1D by $z = 2$ and $\chi = 1/2$. This fixed point is repulsive, i.e., IR unstable. This is schematically depicted in Fig. 1. From a topological viewpoint, it is clear that there should also exist another fixed point, in the limit $g \to \infty$, which is IR unstable (and UV stable). Moreover, let us emphasize that the inviscid limit is equivalent to the limit $g \to \infty$. It is therefore plausible that this third fixed point governs the KPZ equation in this limit, and we call it the inviscid Burgers (IB) fixed point. We show in this Letter that it is indeed the case, and that this fixed point yields $z = 1$. Since it is genuinely nonperturbative, a method such as the FRG is required to study it.

Functional renormalization group for the KPZ equation.—The FRG is a modern and powerful implementation of the RG, which allows for both functional and nonperturbative calculations [24], and is widely used in many domains [25,26]. For the KPZ equation, the FRG yields the strong-coupling fixed point describing the KPZ rough phase in any dimension [27], whereas perturbation theory, even resummed to all orders, fails to access it in $d \geq 2$ [28]. In 1D, the scaling function associated with the two-point correlation function calculated from FRG compares at a high precision level with the exact result [29]. Moreover, it can be extended to arbitrary dimensions where it allowed for the calculation of the scaling function and other properties in $d > 1$ [30–32]. We thus employ this method to investigate the IB fixed point.

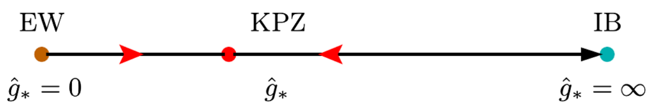

FIG. 1. The three fixed points of the KPZ equation, the KPZ one, which is IR stable, and the EW and IB ones, which are both IR unstable, UV stable. Red arrows indicate the RG flow.

The starting point of the FRG is the KPZ field theory, which can be obtained from a standard procedure introducing a response field $\tilde{h}$ [33–36], and reads

$$\mathcal{Z}[\mathcal{J}] = \int \mathcal{D}h\mathcal{D}\tilde{h}e^{-\mathcal{S}_{\rm KPZ}[\varphi]+\int_{t,\mathbf{x}}\mathcal{J}\cdot\varphi}$$

$$\mathcal{S}_{\rm KPZ}[\varphi] = \int_{t,\mathbf{x}}\left\{\tilde{h}\left[\partial_t h - \nu\nabla^2 h - \frac{\lambda}{2}(\boldsymbol{\nabla}h)^2\right] - D\tilde{h}^2\right\}, \qquad (2)$$

where $\varphi = (h,\tilde{h})$, $\mathcal{J} = (J,\tilde{J})$ are the sources, and $\int_{t,\mathbf{x}} \equiv \int dt d^d\mathbf{x}$ [37]. The FRG formalism consists in *progressively* integrating the fluctuations in $\mathcal{Z}$, by suppressing the contribution of low wave number modes $q = |\mathbf{q}| \lesssim \kappa$, where κ is the RG scale, in the functional integral. This is achieved by adding to $\mathcal{S}_{\rm KPZ}$ a quadratic term of the form $\Delta\mathcal{S}_\kappa[\varphi] = \frac{1}{2}\int\varphi_i\mathcal{R}_{\kappa,ij}\varphi_j$, where $\mathcal{R}_\kappa$ is a 2×2 matrix, whose elements $\mathcal{R}_{\kappa,ij}$ are called cut-off functions or regulators. They are required to be large $\mathcal{R}_{\kappa,ij}(\mathbf{q}) \sim \kappa^2$ at low wave numbers $q \lesssim \kappa$ such that these modes are damped in the functional integral, and to vanish $\mathcal{R}_{\kappa,ij}(\mathbf{q}) = 0$ at high wave numbers $q \gtrsim \kappa$ such that these modes are unaffected. Its precise form is unimportant (we refer to [38] for technical details, which also includes the additional Refs. [39–50]). In the presence of $\Delta\mathcal{S}_\kappa$, $\mathcal{Z}$ becomes κ dependent, and one defines the effective average action Γ_κ, as the Legendre transform of $\mathcal{W}_\kappa = \ln\mathcal{Z}_\kappa$, i.e., $\Gamma_\kappa = -\mathcal{W}_\kappa + \int_{t,\mathbf{x}}\mathcal{J}\cdot\psi - \Delta\mathcal{S}[\psi]$, where $\Psi = (\psi,\tilde{\psi}) = \langle\varphi\rangle$. The $\Delta\mathcal{S}[\psi]$ term, with the requirement that the cutoff functions diverge at the microscopic scale $\kappa = \Lambda$ and vanish at $\kappa = 0$, ensures that Γ_κ identifies with the microscopic KPZ action (2) at $\kappa = \Lambda$, and becomes the full Γ, which encompasses all the statistical properties of the system, in the limit $\kappa \to 0$. The evolution of Γ_κ with the RG scale in between these two scales is given by the Wetterich exact RG equation [24]

$$\partial_\kappa\Gamma_\kappa = \frac{1}{2}\mathrm{Tr}\int\partial_\kappa\mathcal{R}_\kappa\cdot G_\kappa, \qquad G_\kappa \equiv \left[\Gamma_\kappa^{(2)} + \mathcal{R}_\kappa\right]^{-1}, \qquad (3)$$

where $\Gamma_\kappa^{(2)}$ is the Hessian of Γ_κ. The power of the FRG formalism is that this equation can be solved using nonperturbative and functional approximation schemes [26].

Flow diagram of the 1D KPZ equation.—Let us confirm the existence of the IB fixed point. For this, the simplest approximation, which consists in considering the flow of the original parameters ν, λ, and D only, suffices. The corresponding ansatz for Γ_κ reads

$$\Gamma_\kappa = \int_{t,\mathbf{x}}\left\{\tilde{\psi}\left[\partial_t\psi - \nu_\kappa\nabla^2\psi - \frac{\lambda_\kappa}{2}(\boldsymbol{\nabla}\psi)^2\right] - D_\kappa\tilde{\psi}^2\right\}. \qquad (4)$$

From this ansatz, one deduces, measuring in units of κ, that the frequency scales as $\omega \sim \kappa^2 \nu_\kappa$, and that the fields have scaling dimensions $[\tilde{\psi}] = (\kappa^{d+2} D_\kappa^{-1} \nu_\kappa)^{1/2}$ and $[\psi] = (\kappa^{d-2} D_\kappa \nu_\kappa^{-1})^{1/2}$. One can show that the coupling λ is not renormalized, i.e., $\lambda_\kappa = \lambda$ at all scales, due to the statistical tilt symmetry of the KPZ equation, or equivalently the Galilean invariance of the Burgers equation [29,51]. Defining the anomalous dimensions $\eta_\kappa^\nu = -\partial_s \ln \nu_\kappa$ and $\eta_\kappa^D = -\partial_s \ln D_\kappa$, with $s = \ln(\kappa/\Lambda)$ the RG "time," one deduces that the critical exponents are obtained as $z = 2 - \eta_*^\nu$ and $\chi = (2 - d - \eta_*^\nu + \eta_*^D)/2$, where $_*$ denotes fixed-point values [27]. One then defines the dimensionless effective coupling $\hat{g}_\kappa = \kappa^{d-2} \lambda^2 D_\kappa / \nu_\kappa^3$. Its flow equation is given by $\partial_s \hat{g}_\kappa = \hat{g}_\kappa (d - 2 - \eta_\kappa^D + 3\eta_\kappa^\nu)$. The expressions of η_κ^ν and η_κ^D are obtained from projecting the exact flow equation (3) onto the ansatz (4). The calculation is detailed in [38]. At a finite fixed point $0 < \hat{g}_* < \infty$, one thus finds the exact identity $z + \chi = 2$, whereas the exponent values are not constrained if $\hat{g}_*$ vanishes or diverges. Moreover, in 1D, the accidental time-reversal symmetry further imposes that $D_\kappa = \nu_\kappa$ [29,51], and thus $\eta_\kappa^D = \eta_\kappa^\nu \equiv \eta_\kappa$, which leads to $\chi = \eta_* = 1/2$. We require this symmetry to be preserved for all values of ν, such that the inviscid limit corresponds to a joined limit $\nu \to 0$, $D \to 0$ with ν/D fixed, as in [17]. This yields that the stationary solution is a Brownian in space and $\chi = 1/2$ for all ν. The flow equation for $\hat{g}_\kappa$ also possesses the two fixed-point solutions $\hat{g}_* = 0$ and $\hat{g}_* = \infty$. In order to render this more explicit, let us change the variable to $\hat{w}_\kappa = \hat{g}_\kappa / (1 + \hat{g}_\kappa)$. The flow equation for $\hat{w}_\kappa$ reads $\partial_s \hat{w}_\kappa = \hat{w}_\kappa (1 - \hat{w}_\kappa)(2\eta_\kappa - 1)$. The explicit equation for η_κ can be found in [38], which shows that it vanishes for $\hat{w}_\kappa = 0$. It is manifest that this equation possesses the three following fixed-point solutions: (i) EW with $\hat{w}_* = 0$, $\eta_* = 0$ and thus $z_{\rm EW} = 2$, (ii) KPZ with $0 < \hat{w}_* < 1$, $\eta_* = 1/2$ and thus $z_{\rm KPZ} = 3/2$, (iii) IB with $\hat{w}_* = 1$. However, η_* is not fixed in this case by the fixed point condition $\partial_s \hat{w}_\kappa = 0$ and has to be calculated from the flow. While it provides the confirmation of the scenario schematically depicted on Fig. 1, this simple approximation is not sufficient to reliably conclude on the value of $z_{\rm IB}$ (see [38]). We now show how to determine this value.

FRG flow equations within the NLO approximation.—In order to have a quantitative description of the three fixed points, we resort to a refined approximation, introduced in [30] and called next-to-leading-order (NLO) approximation. The NLO ansatz consists in replacing in (4) the effective parameters ν_κ and D_κ by full effective functions $f_\kappa^\nu(\omega, p)$ and $f_\kappa^D(\omega, p)$, respectively. In 1D, the time-reversal symmetry imposes $f_\kappa^\nu = f_\kappa^D \equiv f_\kappa(\omega, p)$, and there is only one anomalous dimension $\eta_\kappa = -\partial_s \ln D_\kappa$. The corresponding NLO equations are derived in [38]. We numerically solve the flow equation for the dimensionless function $\hat{f}_\kappa(\hat{\omega}, \hat{p}) = f_\kappa(\omega/(\kappa^2 D_\kappa), p/\kappa)/D_\kappa$, together with the equation for $\hat{g}_\kappa$ and η_κ, on a discretized grid $(\hat{\omega}, \hat{p})$ starting from the initial condition $\hat{f}_\Lambda(\hat{\omega}, \hat{p}) = 1$ and $\hat{g}_\Lambda$ at the microscopic scale $\kappa = \Lambda$. The numerical integration is detailed in [38]. For any initial value $\hat{g}_\Lambda$, the flow reaches in the IR the KPZ fixed point. One can compute from it the correlation function $\bar{C}(\varpi, p) = \mathcal{F}[\langle (h(t', \mathbf{x}') - h(t, \mathbf{x}))^2 \rangle]$ (with $\mathcal{F}$ the Fourier transform) as $\bar{C}(\hat{\varpi}, \hat{p}) = 2\hat{f}_*(\hat{\varpi}, \hat{p}) / (\hat{\varpi}^2 + \hat{p}^4 \hat{f}_*{}^2(\hat{\varpi}, \hat{p}))$. The dynamical exponent can be probed through the half-frequency, defined as $\hat{C}(\hat{\varpi}_{1/2}(p), \hat{p}) = \hat{C}(0, \hat{p})/2$, which shows the expected KPZ scaling $\varpi_{1/2} \sim \hat{p}^{3/2}$. Fourier transforming the correlation function back in time, one obtains that the data for $C(\hat{t}, \hat{p})/C(0, \hat{p})$ all collapse onto a single curve when plotted as a function of $pt^{2/3}$, which defines the universal KPZ scaling function. We show in Fig. 2 that the NLO scaling function compares accurately with the exact result from [16]. It reproduces in particular the negative dip

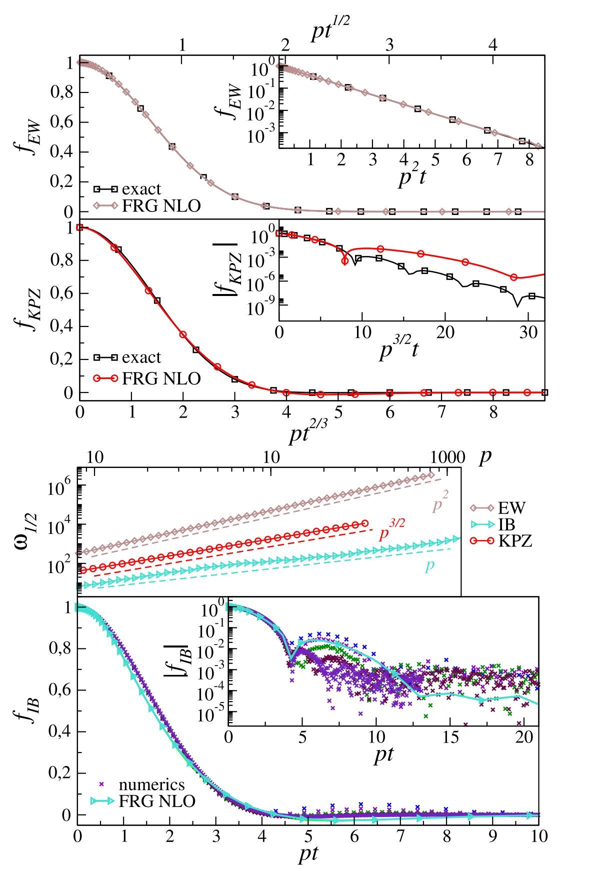

FIG. 2. Results from the numerical integration of the FRG flow equations within the NLO approximation, obtained from the UV flow at either small (EW) or large (IB) initial coupling $\hat{g}_\Lambda$, and from the IR fixed point (KPZ). Half-frequency $\omega_{1/2}$ (shifted vertically for visibility) as a function of p, showing the three dynamical scaling exponents $z = 3/2$ for KPZ, $z = 2$ for EW, and $z = 1$ for IB. Associated scaling functions $f_{\rm KPZ}$, $f_{\rm EW}$, and $f_{\rm IB}$, compared respectively with the exact results from [16], with the analytical solution [38], and with numerical simulations from [17].

followed by a stretched exponential tail with superimposed oscillations.

Although the flow always reaches in the IR the KPZ fixed point, irrespectively of the initial value of $\hat{g}_\Lambda$, the beginning of the flow, referred to as the UV flow, is sensitive to it. For small initial values $\hat{g}_\Lambda \ll \hat{g}_*$, the UV flow is dominated by the EW fixed point, while for large $\hat{g}_\Lambda \gg \hat{g}_*$, it is controlled by the IB one. We compute the corresponding correlation functions, half-frequency, and scaling functions by focusing on the UV flow starting from either $\hat{g}_\Lambda = 10^{-4}$ or $\hat{g}_\Lambda = 10^4$. The results are displayed in Fig. 2. The half-frequency clearly shows two other scaling regimes besides the KPZ one, which are $z = 2$ for EW, and $z = 1$ for IB. The EW scaling function exactly matches the expected result [38] up to numerical precision. The IB scaling function is in close agreement with the data from the simulations of [17], at least for $pt \lesssim 4$, featuring in particular the observed negative dip [38]. This confirms that the IB fixed point indeed yields a critical exponent $z = 1$. We have thus unveiled the theoretical origin of the missing scaling.

Exact asymptotic form of the IB scaling function.—The previous results were derived within the NLO approximation of the FRG. We now show that we can in fact prove the $z = 1$ scaling in the UV, and obtain an exact asymptotic form of the scaling function, by considering the limit of large wave number p. The proof is in close analogy with the derivation presented in [52–54] for the Navier-Stokes (NS) equation. In this case, it was shown that the flow equation for any n-point correlation function $C^{(n)}$ can be closed exactly in the limit of large wave numbers $p_i = |\mathbf{p}_i|$. The closure relies on two fundamental ingredients. The first one is the presence of $\partial_\kappa \mathcal{R}_\kappa$ in the exact FRG flow equations, which ensures that they can be safely expanded in the limit of large p_i (see [38] for details). The second one is the existence of extended symmetries, which exactly fix the expression of the expanded vertices entering the flow equation at large p_i. Moreover, it turns out that the resulting closed flow equation for any $C^{(n)}$ can be solved at the fixed point. This solution gives the exact time dependence of $C^{(n)}(\{t_i, \mathbf{p}_i\}_{i=1,n})$ in the limit of large p_i [53]. These results were precisely confirmed for the two- and three-point functions by direct numerical simulations [55,56]. Moreover, these simulations showed that the regime of validity of the large p expansion starts at wave numbers larger, but not too far from the inverse integral scale, which means that it encompasses wave numbers within the universal inertial range down to the dissipative range.

To simply exploit the analogy with the NS case, let us consider the action for the Burgers equation in 1D

$$\mathcal{S}_{\text{Burgers}} = \int_{t,x} \Big\{ \bar{v} \Big[\partial_t v + v \partial_x v - \nu \partial_x^2 v \Big] - D(\partial_x \bar{v})^2 \Big\},$$

where the form of the noise follows from the mapping with the KPZ equation [57,58]. This action shares with the NS one an extended symmetry which is the time-dependent Galilean symmetry: $(t, \mathbf{x}, \mathbf{v}) \to (t, \mathbf{x} + \mathbf{e}(t), \mathbf{v} - \dot{\mathbf{e}}(t))$, where $\mathbf{e}(t)$ is an arbitrary infinitesimal time-dependent vector. Indeed, this transformation does not leave the Burgers or NS actions strictly invariant, but their variations are *linear* in the fields. In such a case, one can derive exact relations, called Ward identities, amongst the vertices $\Gamma^{(n)}$. The Ward identities for the Galilean extended symmetry entail that each n-point vertex with a zero-wave vector associated with a velocity field is exactly given in terms of $(n-1)$-point vertices [38,53,59]. It turns out that in 1D, the Burgers action also admits a time-dependent shift symmetry, which is simply $\bar{v} \to \bar{v} + \bar{e}(t)$. This only holds in 1D because the advection term can be written in this dimension only as a total derivative. This extended symmetry also yields a set of exact Ward identities, which entail that each n-point vertex with a zero-wave vector associated with a response velocity field exactly vanishes. All these identities are explicitly derived in [38].

After a calculation, reported in [38], which is lengthy but very similar to [52], one obtains that the flow equation for the two-point function $C_\kappa(t, p)$ is exactly closed in the limit of large p. Moreover, it can be solved at the fixed point, leading to the explicit form

$$C(t,p) = C(0,p) \times \begin{cases} \exp(-\mu_0 (pt)^2) & t \ll \tau \\ \exp(-\mu_\infty p^2 |t|) & t \gg \tau \end{cases}, \quad (5)$$

where μ_0, μ_∞ are nonuniversal constants, and τ is a typical timescale [38]. Let us first focus on the small time expression. It shows that the data for $C(t,p)/C(0,p)$ should collapse when plotted as a function of pt. Thus, it demonstrates the $z = 1$ dynamical scaling exponent. This behavior is reminiscent of the effect of random sweeping in 3D turbulence, although for the 1D Burgers equation, the large scales do not dominate. Furthermore, it gives the asymptotic form of the associated scaling function, which is simply a Gaussian. This result is compared in Fig. 3 with the data from the numerical simulations of [17], using μ_0 as a fitting

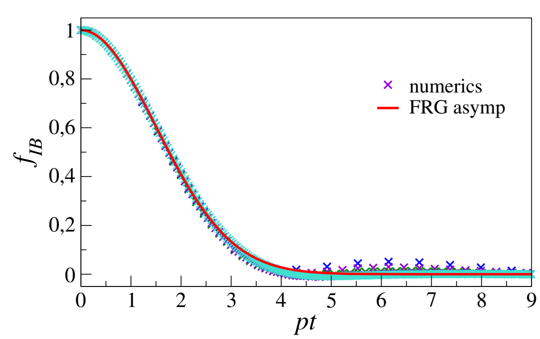

FIG. 3. Asymptotic form of the IB scaling function obtained from the solution of the exact FRG flow equation at large wave number and small time, compared with the numerics from [17].

parameter. The numerical data are accurately described by the Gaussian, as was already argued in [17], at small $pt \lesssim 4$, before the negative dip which is not featured by the Gaussian, but is reproduced by the NLO solution. Let us now turn to the large time behavior. In the numerical data, the initial Gaussian decay is such that the scaling function rapidly reaches numerical noise level, preventing one from resolving the large time regime and accessing the crossover at large time. However, one can notice that the quality of the collapse deteriorates at large $pt \gtrsim 4$, which signals a change of behavior, as expected from the theoretical prediction (5) of a $p^2 t$ scaling at large time. This would require a better resolution to be further investigated.

Conclusion.—We have shown that the 1D KPZ equation, although exactly solvable, still reveals unforseen features, as we demonstrated the emergence of a new scaling $z = 1$. This scaling arises from the inviscid Burgers fixed point which, although unstable in the IR, controls the UV behavior of the correlation function when the initial nonlinearity is large enough. We established this scaling by numerically solving the FRG flow equations within the NLO approximation, and by obtaining the exact asymptotic form of the correlation function in the limit of a large wave number.

The probability distributions of height fluctuations are not easily accessible within the FRG formalism. The distributions in the inviscid limit have been studied numerically in [17,19] which showed that they are non-Gaussian, but differ from the Tracy-Widom distributions expected at the KPZ fixed point. We hope our findings will trigger new works to obtain exact results on the distributions at the new fixed point. They also open up uncharted territory, which is the UV, or large nonlinearity, scaling behavior of the KPZ equation in higher dimensions.

The authors thank B. Delamotte and N. Wschebor for enlightening discussions. L. C. acknowledges support from the French ANR through the project NeqFluids (Grant No. ANR-18-CE92-0019) and support from Institut Universitaire de France (IUF). F. V. acknowledges support from QuantForm-UGA (Grant No. ANR-21-CMAQ-003).

C. F. and F. V. contributed equally to this work.

[1] M. Kardar, G. Parisi, and Y.-C. Zhang, Dynamic scaling of growing interfaces, Phys. Rev. Lett. **56**, 889 (1986).
[2] J. Maunuksela, M. Myllys, O.-P. Kähkönen, J. Timonen, N. Provatas, M. J. Alava, and T. Ala-Nissila, Kinetic roughening in slow combustion of paper, Phys. Rev. Lett. **79**, 1515 (1997).
[3] M. A. C. Huergo, M. A. Pasquale, P. H. González, A. E. Bolzán, and A. J. Arvia, Growth dynamics of cancer cell colonies and their comparison with noncancerous cells, Phys. Rev. E **85**, 011918 (2012).
[4] T. M. Jun-ichi Wakita, Hiroto Itoh, and M. Matsushita, Self-affinity for the growing interface of bacterial colonies, J. Phys. Soc. Jpn. **66**, 67 (1997).
[5] S. Najem, A. Krayem, T. Ala-Nissila, and M. Grant, Kinetic roughening of the urban skyline, Phys. Rev. E **101**, 050301 (R) (2020).
[6] M. Kardar, Replica Bethe ansatz studies of two-dimensional interfaces with quenched random impurities, Nucl. Phys. **B290**, 582 (1987).
[7] J. Burgers, *A Mathematical Model Illustrating the Theory of Turbulence* (Elsevier, New York, 1948), pp. 171–199, 10.1016/S0065-2156(08)70100-5.
[8] Q. Fontaine, D. Squizzato, F. Baboux, I. Amelio, A. Lemaître, M. Morassi, I. Sagnes, L. Le Gratiet, A. Harouri, M. Wouters, I. Carusotto, A. Amo, M. Richard, A. Minguzzi, L. Canet, S. Ravets, and J. Bloch, Kardar–Parisi–Zhang universality in a one-dimensional polariton condensate, Nature (London) **608**, 687 (2022).
[9] D. Wei, A. Rubio-Abadal, B. Ye, F. Machado, J. Kemp, K. Srakaew, S. Hollerith, J. Rui, S. Gopalakrishnan, N. Y. Yao, I. Bloch, and J. Zeiher, Quantum gas microscopy of Kardar-Parisi-Zhang superdiffusion, Science **376**, 716 (2022).
[10] A. Scheie, N. E. Sherman, M. Dupont, S. E. Nagler, M. B. Stone, G. E. Granroth, J. E. Moore, and D. A. Tennant, Detection of Kardar–Parisi–Zhang hydrodynamics in a quantum Heisenberg spin-1/2 chain, Nat. Phys. **17**, 726 (2022).
[11] T. Halpin-Healy and Y.-C. Zhang, Kinetic roughening phenomena, stochastic growth, directed polymers and all that. Aspects of multidisciplinary statistical mechanics, Phys. Rep. **254**, 215 (1995).
[12] J. Krug, Origins of scale invariance in growth processes, Adv. Phys. **46**, 139 (1997).
[13] T. Halpin-Healy and K. A. Takeuchi, A KPZ cocktail-shaken, not stirred..., J. Stat. Phys. **160**, 794 (2015).
[14] K. A. Takeuchi, An appetizer to modern developments on the Kardar–Parisi–Zhang universality class, Physica (Amsterdam) **504A**, 77 (2018).
[15] I. Corwin, The Kardar-Parisi-Zhang equation and universality classes, Random Matrices Theory Appl. **01**, 1130001 (2012).
[16] M. Prähofer and H. Spohn, Exact scaling functions for one-dimensional stationary KPZ growth, J. Stat. Phys. **115**, 255 (2004).
[17] C. Cartes, E. Tirapegui, R. Pandit, and M. Brachet, The Galerkin-truncated Burgers equation: Crossover from inviscid-thermalized to Kardar–Parisi–Zhang scaling, Phil. Trans. R. Soc. A **380**, 20210090 (2022).
[18] J. Bec and K. Khanin, Burgers turbulence, Phys. Rep. **447**, 1 (2007).
[19] E. Rodríguez-Fernández, S. N. Santalla, M. Castro, and R. Cuerno, Anomalous ballistic scaling in the tensionless or inviscid Kardar-Parisi-Zhang equation, Phys. Rev. E **106**, 024802 (2022).
[20] K. Fujimoto, R. Hamazaki, and Y. Kawaguchi, Family-Vicsek scaling of roughness growth in a strongly interacting Bose gas, Phys. Rev. Lett. **124**, 210604 (2020).
[21] S. F. Edwards and D. R. Wilkinson, The surface statistics of a granular aggregate, Proc. R. Soc. A **381**, 17 (1982).
[22] A. J. Majda and I. Timofeyev, Remarkable statistical behavior for truncated Burgers–Hopf dynamics, Proc. Natl. Acad. Sci. U.S.A. **97**, 12413 (2000).

[23] K. G. Wilson and J. Kogut, The renormalization group and the ϵ expansion, Phys. Rep. **12**, 75 (1974).
[24] C. Wetterich, Exact evolution equation for the effective potential, Phys. Lett. B **301**, 90 (1993).
[25] J. Berges, N. Tetradis, and C. Wetterich, Non-perturbative renormalization flow in quantum field theory and statistical physics, Phys. Rep. **363**, 223 (2002).
[26] N. Dupuis, L. Canet, A. Eichhorn, W. Metzner, J. Pawlowski, M. Tissier, and N. Wschebor, The nonperturbative functional renormalization group and its applications, Phys. Rep. **910**, 1 (2021).
[27] L. Canet, H. Chaté, B. Delamotte, and N. Wschebor, Nonperturbative renormalization group for the Kardar-Parisi-Zhang equation, Phys. Rev. Lett. **104**, 150601 (2010).
[28] K. J. Wiese, On the perturbation expansion of the KPZ equation, J. Stat. Phys. **93**, 143 (1998).
[29] L. Canet, H. Chaté, B. Delamotte, and N. Wschebor, Nonperturbative renormalization group for the Kardar-Parisi-Zhang equation: General framework and first applications, Phys. Rev. E **84**, 061128 (2011).
[30] T. Kloss, L. Canet, and N. Wschebor, Nonperturbative renormalization group for the stationary Kardar-Parisi-Zhang equation: Scaling functions and amplitude ratios in $1+1$, $2+1$, and $3+1$ dimensions, Phys. Rev. E **86**, 051124 (2012).
[31] T. Kloss, L. Canet, B. Delamotte, and N. Wschebor, Kardar-Parisi-Zhang equation with spatially correlated noise: A unified picture from nonperturbative renormalization group, Phys. Rev. E **89**, 022108 (2014).
[32] D. Squizzato and L. Canet, Kardar-Parisi-Zhang equation with temporally correlated noise: A nonperturbative renormalization group approach, Phys. Rev. E **100**, 062143 (2019).
[33] P. C. Martin, E. D. Siggia, and H. A. Rose, Statistical dynamics of classical systems, Phys. Rev. A **8**, 423 (1973).
[34] H.-K. Janssen, On a Lagrangean for classical field dynamics and renormalization group calculations of dynamical critical properties, Z. Phys. B **23**, 377 (1976).
[35] C. de Dominicis, Techniques de renormalisation de la théorie des champs et dynamique des phénomènes critiques, J. Phys. (Paris), Colloq. **37**, 247 (1976).
[36] F. Langouche, D. Roekaerts, and E. Tirapegui, Functional integral methods for stochastic fields, Physica (Amsterdam) **95A**, 252 (1979).
[37] Note that we implicitly used Itō's discretization such that the functional determinant is unity (see [38]).
[38] See Supplemental Material at http://link.aps.org/supplemental/10.1103/PhysRevLett.131.247101 for details.
[39] U. C. Täuber, *Critical Dynamics: A Field Theory Approach to Equilibrium and Non-Equilibrium Scaling Behavior* (Cambridge University Press, Cambridge, 2014), 10.1017/CBO9781139046213.
[40] L. Canet, H. Chaté, and B. Delamotte, General framework of the non-perturbative renormalization group for non-equilibrium steady states, J. Phys. A **44**, 495001 (2011).
[41] T. Halpin-Healy, Extremal paths, the stochastic heat equation, and the three-dimensional Kardar-Parisi-Zhang universality class, Phys. Rev. E **88**, 042118 (2013); Phys. Rev. E **88**, 069903(E) (2013).
[42] K. Deligiannis, Q. Fontaine, D. Squizzato, M. Richard, S. Ravets, J. Bloch, A. Minguzzi, and L. Canet, Kardar-Parisi-Zhang universality in discrete two-dimensional driven-dissipative exciton polariton condensates, Phys. Rev. Res. **4**, 043207 (2022).
[43] L. T. Adzhemyan, N. V. Antonov, and A. N. Vasil'ev, *The Field Theoretic Renormalization Group in Fully Developed Turbulence* (Gordon and Breach, London, 1999), https://zbmath.org/0956.76002.
[44] N. V. Antonov, S. V. Borisenok, and V. I. Girina, Renormalisation Group approach in the theory of fully developed turbulence. Composite operators of canonical dimension 8, Theor. Math. Phys. **106**, 75 (1996).
[45] A. Berera and D. Hochberg, Gauge symmetry and Slavnov-Taylor identities for randomly stirred fluids, Phys. Rev. Lett. **99**, 254501 (2007).
[46] J.-P. Blaizot, R. Méndez-Galain, and N. Wschebor, A new method to solve the non-perturbative renormalization group equations, Phys. Lett. B **632**, 571 (2006).
[47] J.-P. Blaizot, R. Méndez-Galain, and N. Wschebor, Non-perturbative renormalization group calculation of the scalar self-energy, Eur. Phys. J. B **58**, 297 (2007).
[48] F. Benitez, J.-P. Blaizot, H. Chaté, B. Delamotte, R. Méndez-Galain, and N. Wschebor, Nonperturbative renormalization group preserving full-momentum dependence: Implementation and quantitative evaluation, Phys. Rev. E **85**, 026707 (2012).
[49] L. Canet, V. Rossetto, N. Wschebor, and G. Balarac, Spatiotemporal velocity-velocity correlation function in fully developed turbulence, Phys. Rev. E **95**, 023107 (2017).
[50] M. Tarpin, L. Canet, C. Pagani, and N. Wschebor, Stationary, isotropic and homogeneous two-dimensional turbulence: A first non-perturbative renormalization group approach, J. Phys. A **52**, 085501 (2019).
[51] E. Frey and U. C. Täuber, Two-loop renormalization-group analysis of the Burgers–Kardar-Parisi-Zhang equation, Phys. Rev. E **50**, 1024 (1994).
[52] L. Canet, B. Delamotte, and N. Wschebor, Fully developed isotropic turbulence: Nonperturbative renormalization group formalism and fixed-point solution, Phys. Rev. E **93**, 063101 (2016).
[53] M. Tarpin, L. Canet, and N. Wschebor, Breaking of scale invariance in the time dependence of correlation functions in isotropic and homogeneous turbulence, Phys. Fluids **30**, 055102 (2018).
[54] L. Canet, Functional renormalisation group for turbulence, J. Fluid Mech. **950**, P1 (2022).
[55] A. Gorbunova, G. Balarac, L. Canet, G. Eyink, and V. Rossetto, Spatio-temporal correlations in three-dimensional homogeneous and isotropic turbulence, Phys. Fluids **33**, 045114 (2021).
[56] A. Gorbunova, C. Pagani, G. Balarac, L. Canet, and V. Rossetto, Eulerian spatiotemporal correlations in passive scalar turbulence, Phys. Rev. Fluids **6**, 124606 (2021).
[57] Note that the Burgers equation was also studied using FRG in [58].
[58] S. Mathey, T. Gasenzer, and J. M. Pawlowski, Anomalous scaling at nonthermal fixed points of Burgers' and Gross-Pitaevskii turbulence, Phys. Rev. A **92**, 023635 (2015).
[59] L. Canet, B. Delamotte, and N. Wschebor, Fully developed isotropic turbulence: Symmetries and exact identities, Phys. Rev. E **91**, 053004 (2015).